Se Changed the Component of Organic Chemicals and Cr bioavailability in Pak Choi Rhizosphere Soil Contaminated with Cr

Miaomiao Cai
Huazhong Agricultural University: Huazhong Agriculture University
Xiaohu Zhao (xhzhao@mail.hzau.edu.cn)
Huazhong Agricultural University College of Resources and Environment https://orcid.org/0000-0002-6641-8819
Xu Wang
Guangdong Academy of Agricultural Sciences
Guangyu Shi
Suzhou University of Science and Technology
Chengxiao Hu
Huazhong Agricultural University: Huazhong Agriculture University

Research Article

Keywords: chromium, selenium, metabolites, rhizosphere, absorption

Posted Date: February 8th, 2021

DOI: https://doi.org/10.21203/rs.3.rs-161205/v1

Version of Record: A version of this preprint was published at Environmental Science and Pollution Research on July 10th, 2021. See the published version at https://doi.org/10.1007/s11356-021-13465-w.

Se changed the component of organic chemicals and Cr bioavailability in pak choi rhizosphere soil contaminated with Cr

Miaomiao Cai [1, a], Xiaohu Zhao [1, a], Xu Wang [b], Guangyu Shi [c], Chengxiao Hu [a *]

[a] College of Resources and Environment, Huazhong Agricultural University / Hubei Provincial Engineering Laboratory for New-Type Fertilizer / Research Center of Trace Elements / Hubei Key Laboratory of Soil Environment and Pollution Remediation, Wuhan 430070, China

[b] Public Monitoring Center for Agro-product of Guangdong Academy of Agricultural Sciences, Guangzhou 510640, China

[c] College of Environment Science and Engineering, Suzhou University of Science and Technology, Suzhou 215009, China

[1] These authors contributed equally to present work.

* Corresponding author at: College of Resources and Environment, Huazhong Agricultural University, Wuhan 430070, China.

E-mail address: hucx@mail.hzau.edu.cn (C.X. Hu).

Tel/Fax: +86 27 87288730

Abstract: Rhizosphere organic chemicals response and its role on Cr/Se adsorption is of great importance to understand Cr/Se bioavailability in Cr contaminated soil with the application of Se. In the current work, the processes were carried out using rhizobox experiment (*Brassica campestris* L. ssp. *Chinensis* Makino). The results showed that in soil contaminated by 200 mg kg^{-1} Cr(III), Se(IV) complexed with Cr(III) and carboxylic acid (cis-9,10-Epoxystearic acid, hexadecanedioic acid) reduced Cr(VI) to Cr(III), thus increasing of Cr adsorption, furtherly, decreasing Cr bioavailability. While, in soil contaminated by 120 mg kg^{-1} Cr(VI), Se(VI) competed for adsorption sites with Cr(VI) and salicylic acid activated insoluble Cr(III), thus decreasing Cr adsorption, finally, increasing Cr bioavailability. Moreover, with Cr contamination, Se bioavailability in soil was enhanced by the secretion of carboxylic acid, which can reduce Se to lower valent state, compete the adsorption sites and complex with Se oxyanion. These results yielded a better understanding of rhizosphere dynamics regulating by Se application in Cr contaminated soil. Moreover, the current study supplemented the theoretical basis for beneficial elements application as an environment-friendly resource to facilitate cleaner production in heavy metal contaminated soil.

Keywords: chromium, selenium, metabolites, rhizosphere, absorption

1. Introduction

Chromium (Cr), a major inorganic pollutant in the environment, occurs in two stable forms: Cr(III) and Cr(VI), with diverse mobility and bioavailability in the soil (Shahid et al., 2017). Excessive Cr in the growth medium raise various adverse effects on plant physiological metabolism (Qing et al., 2015; Handa et al., 2018a, b). Furtherly, the accumulation of heavy metals in ecological system cause hazardous effects on the entire food chain (Yang et al., 2019). To facilitate cleaner production in Cr contaminated soil environment, environment-friendly measures are necessary to be developed. But the hazardous effects are not determined by the total Cr in soil. In fact, available Cr plays a more important role in regulating the plant growth, Cr accumulation and soil health. Additionally, Cr bioavailability is affected by soil pH, Eh, root exudates, microbe activities and so on (Shahid et al., 2017). Rhizosphere is a highly dynamic micro-environment and is the most closely related to Cr transfer from soil to plant. Importantly, the organic chemicals, including microbial products and root exudates (Bais et al., 2006; Pétriacq et al., 2017), are the intermediates to regulate the chemical behavior of Cr in rhizosphere. Generally, the functional group of organic chemicals, such as carboxyl, hydroxyl and carbonyl, complex with Cr to affect Cr adsorption and activate Cr mobility (Wen et al., 2018). And the organic chemicals act as electron donor for Cr(VI) reduction (Chen et al., 2017; Choppala et al., 2018). Therefore, the changes of organic chemicals are important for Cr bioavailability in rhizosphere soil.

Selenium (Se) is necessary for animal and human beings. It is of great benefit for plant growth and development under heavy metal stress (Ismael et al., 2019). Se alleviated the inhibitory effects on heavy metal induced phytotoxicity to plant by moderating the physiological metabolism, such as enhancing of antioxidative enzyme activity and photosynthesis efficiency, modulating of secondary metabolites content, separating element in vacuole and fixing it on cell wall, and regulating carbohydrate and nitrogen metabolism (Qing et al., 2015; Handa et al., 2018a, b; Zhao et al., 2019a, b). Moreover, Se application in soil increased the pH and transfer heavy metals from soluble form to combined form, thus decreased the mobility of heavy metals in soil and also fixed heavy metals in roots (Wang et al., 2016; Huang et al., 2018; Ismael et al., 2019). This was ascribed to the shifting of soil micro-environment induced by Se addition, especially rhizosphere organic chemicals and microbe activities, which can change heavy metals beheavior in soil. Within a certain range, the higher Se content in soil contained

the higher microbial diversity (Lei et al., 2011; Liu et al., 2019a). Furtherly, our previous study showed that bacterial community shifting induced by Se application regulated Cr bioavailability in Cr contaminated soil and acted as maintainer of soil micro-environment (Cai et al., 2019). In summary, Se in soil performed direct and indirect effects on rhizosphere organic chemicals. For the direct effects, the transfer of Se from the soil to plant altered the root exudates through affecting physiological metabolism. For the indirect effects, Se in soil affected the microorganism development and thus modified the microbial products in rhizosphere (Huang et al., 2009; Rosenfeld et al., 2018; Cai et al., 2019). That was to say that Se has great potential to be exploited as an environment-friendly antidote for plants and a regulator for soil micro-environment under Cr stress. However, it is not clear how Se regulated Cr adsorption and thus bioavailability through influencing rhizosphere organic chemicals components and their functional groups in Cr contaminated soil with plant growth.

Generally, when Se was applied in soil contaminated with heavy metal, the detoxification effects caused by Se were considered as the main subject, and the enhance of Se accumulation in plant was regarded as physiological drive to cope with heavy metal stress (Qing et al., 2015; Handa et al., 2018a, b; Zhao et al., 2019a, b). However, the changes of Se bioavailability in soil, which was ascribed to the changes of soil biochemical properties in heavy metal contaminated soil, was rarely noticed. In rhizosphere soil, heavy metal contamination changed the amounts and species of root exudates, the rhizosphere pH and microbial activities significantly (Zeng et al., 2008; Kılıç et al., 2008; del Real et al., 2017). Additionally, in our previous study, the increase of Se bioavailability in soil was resulted from the decrease of Se reductase relative abundance and increase of soil pH induced by Cr contamination (Cai et al., 2019). That was to say the fluctuation of Se bioavailability induced by heavy metals should be considered as a factor for Se biofortification in heavy metal contaminated soil.

Yet, most studies of root exudates analysis were based on sterile cultivation systems, which could not reflect the rhizosphere organic chemicals actually in the soil environment (Pétriacq et al., 2017; Zhalnina et al., 2018; Zwetsloot et al., 2018). In the current study, rhizobox experiment (*Brassica campestris* L. ssp. *Chinensis* Makino) was conducted, and the concrete objectives were (1) investigating the changes of rhizosphere organic chemicals in Cr contaminated soil with Se application, (2) revealing the mechanisms of Cr adsorption influenced by Se and (3) systematically clarifying how the rhizosphere

processes affected the Cr/Se bioavailability in soil. This study has the implication on the benefit role of Se application in ecological and environmental safety.

2. Materials and Methods

2.1. Experiment preparation and designation.

Soils (0-20 cm) for the present study were collected from Huazhong Agricultural University experimental base (30°28′35″N, 114°21′54″E), Wuhan, China. The collected soils were air-dried and ground (2 mm mesh). The soil properties were displayed in Cai et al. (2019).

The prepared soils were contaminated with Cr(III) (0, 100, 200 mg kg^{-1} soil) or Cr(VI) (60, 120 mg kg^{-1} soil) for more than 30 d in ambient temperature. Chromium (III) trichloride ($CrCl_3$ $3H_2O$) and potassium dichromate (VI) ($K_2Cr_2O_7$) was selected as Cr(III) and Cr(VI) resource, respectively. Se (0, 5 mg kg^{-1}) was mixed in soils using sodium selenite (Na_2SeO_3) with basal fertilizers. Thus, eleven treatments were established as follows with four replications: CK (no plant and no exogenous Cr/Se addition), Cr0Se0, Cr0Se5, Cr(III)100Se0, Cr(III)100Se5, Cr(III)200Se0, Cr(III)200Se5, Cr(VI)60Se0, Cr(VI)60Se5, Cr(VI)120Se0, Cr(VI)120Se5 (the number represents the concentration of the elements, i.e. 120 mg kg^{-1} Cr(VI) + 5 mg kg^{-1} Se).

Pak choi (*Brassica campestris* L. ssp. *Chinensis* Makino) was used in the current study. Before sowing, the seeds were sterilized using 0.5% NaClO solution for 30 min. Each box was sown with three seedlings finally. The rhizoboxes were put under a shed to avoid rain and irrigated as required using deionized water. After 50 d, the plants were harvested.

The designation of the experiment and details of rhizobox were displayed in the previous work of Cai et al. (2019). The soil in the root zone was regarded as rhizosphere soil (RS) and the others in the non-root zone was regarded as bulk soil (BS).

2.2. Root exudates extraction and untargeted metabolic profiling of rhizosphere soils by UPLC-Q-TOF mass spectrometry.

The rhizosphere soils (25 g), stored at -20 °C, were mixed with 20 mL mixture extracting solution (methanol (CH_3OH): acetonitrile (C_2H_3N): distilled water (H_2O) = 2: 2: 1). Then, the soil samples were vortexed for 1 min, ultrasonic extracted for 30 min, revortexed for 1 min and stored at -20 °C for 1 h to precipitate the protein. Next, the mixed samples were centrifuged at 7000 r min^{-1} and 4 °C for 15 min.

The supernatants were filtered through 0.45 μm organic filters. The freeze-dried samples were put in the refrigerator at -80 °C for UPLC-Q-TOF/MS analysis.

For LC-MS analysis, samples were redissolved in 100 μL acetonitrile and water (1: 1, v/v) mixture. To evaluate the repeatability and stability of instrument analysis, quality control (QC) samples were obtained by pooling 5 μL of each sample and analyzed together with the other samples. Analyses were carried out using an UHPLC (1290 Infinity LC, Agilent Technologies) with a quadrupole time–of–flight (AB Sciex TripleTOF 6600). Separation was performed on 2.1 mm × 100 mm ACQUIY UPLC BEH 1.7 μm column (waters, Ireland) with mobile phase containing 25 mM ammonium acetate and 25 mM ammonium hydroxide in water (A) and acetonitrile (B). Then, the ESI source conditions were set according to the previous study (Wen et al., 2019). The ion products were obtained using information dependent acquisition (IDA) with high sensitivity mode. The details were: the collision energy (CE): 35 V with ± 15 eV; declustering potential (DP): ±60 V; exclude isotopes within 4 Da, candidate ions to monitor per cycle: 6. The raw MS data (wiff.scan files) were converted to mzXML files using ProteoWizard MSConvert and processed using XCMS online software. Compounds identification of metabolites were performed by comparing of accuracy m/z value (< 25 ppm) and MS/MS spectra with a laboratory standards database (Shanghai Applied Protein Technology Co., Ltd).

2.3. Qualitative and quantitive analysis of soil organic matter.

The organic matter content of soil samples were determined by wet digestion with potassium dichromate (Bao et al. 2000). The FTIR spectra of soil samples were analyzed with a spectrometer (VERTEX 70). The soil samples (2 mg) from rhizobox experiment and KBr (200 mg) were mixed with the ratio 1: 100 (m/m) and finely ground in an agate mortar. 200 mg mixtures were pressed into a slice for FTIR analysis with four replicates per treatments. The spectras in the range of 4000-400 cm^{-1} with 64 scans per sample and resolution of 4 cm^{-1} were recorded. The spectra data were processed using OMNIC 8.2 (Thermo Scientic, Waltham, MA) with smooth and baseline correction.

2.4. Sorption experiment.

To evaluate adsorption isotherms of Cr in soils (Cr0Se0 (RS, BS), Cr0Se5 (RS, BS)), 2.0 g soil were shaken for 24 h with 20 mL 0.01 mol L^{-1} KNO_3 solutions containing 0, 20, 100, 200, 500, 1000, 1500 mg L^{-1} Cr. $Cr(NO_3)_3$ $9H_2O$ and $K_2Cr_2O_7$ were used as Cr(III) and Cr(VI) resource respectively. Then, the suspensions were centrifuged at 25 °C and the supernatants were filtered through 0.45 μm filters. The

175 samples were digested with acid mixtures (HNO_3: $HClO_4$ = 9:1(v/v)). The concentrations of Cr were
176 determined using flame atomic-absorption spectrometry (AAS, Z-2000; HITACHI, Kyoto, Japan).

177 To evaluate adsorption isotherms of Se in soils (Cr0Se0 (RS, BS), Cr(III)200Se0 (RS, BS),
178 Cr(VI)120Se0 (RS, BS)), 2.0 g soil were shaken for 24 h with 20 mL 0.01 mol L^{-1} KNO_3 solutions
179 containing 0, 1, 2, 4, 6, 8, 10 mg L^{-1} Se. Na_2SeO_3 was used as selenite resource. Then, the suspensions
180 were centrifuged at 25 °C and the supernatants were filtered through 0.45 μm filters. The samples were
181 digested with acid mixtures (HNO_3: $HClO_4$ = 9:1(v/v)). The concentration of Se were measured using
182 atomic fluorescence spectrometry (AFS, Jitian, Beijing, China).

183 The amount of Cr/Se adsorbed was calculated using the following equation:

184 $$S = \frac{(C_0 - C_e)V}{W} \quad (1)$$

185 Where S represents the amount sorbed (mg kg^{-1}), C_0 represents the initial concentration of the
186 elements (mg L^{-1}), Ce represents the equilibrium concentration (mg L^{-1}), V represents the solution
187 volume (mL), and W represents the weight of the soil sample (g).

188 Langmuir isotherm model (Eq. (2)) and Freundlich (Eq. (3)) were used as equation fitting for the
189 isotherm data (Fernández-Pazos et al., 2013; Choppala et al., 2018).

190 $$S = \frac{bq_mC_e}{(1 + bC_e)} \quad (2)$$

191 $$S = KC_e^{(1/n)} \quad (3)$$

192 Where S represents the amount sorbed (mg kg^{-1}), Ce represents the equilibrium concentration (mg
193 L^{-1}), b represents the binding constant that indicates the relative rates of sorption at equilibrium, q_m
194 represents the maximum soil sorption capacity (mg kg^{-1}), K represents the sorption coefficient (L kg^{-1}),
195 and 1/n represents the empirical parameters related to adsorption capacity.

196 *2.5. Statistical analysis.*

197 All the experiments were conducted with four replicates. The non–linear fitting of adsorption
198 experimental data to the different models were performed using OriginPro 2017 (OriginLab,
199 Northampton, Massachusetts, USA).

For rhizosphere chemicals analysis, after normalized to total peak intensity, an orthogonal partial least-squares discriminant analysis (OPLS–DA) was performed using SIMCA–P (version 14.1, Umetrics, Umea, Sweden). To evaluate the robustness of the model, the 7-fold cross-validation and response permutation testing was used in the data analysis. In the OPLS–DA model, the variable importance in the projection (VIP) value of each variable was used to represent its importance for the classification. Metabolites with the VIP value >1 were further used in Student's T-test ($p < 0.05$) at an univariate level to indicate the statistical difference among the two treatments.

3. Results

3.1. Rhizosphere organic chemicals components in Cr contaminated soil with Se application.

To investigate the changes of organic profiles in the rhizosphere, UPLC-Q-TOF/MS technology was used in the present work. In the metabolic profiling of the soils, the total number of peaks picked by XCMS was 1896 and 1703 in the positive and negative ion modes, respectively.

To show the difference of rhizosphere organic chemicals after Se application, the criteria in OPLS-DA model, VIP > 1 and *p*-value < 0.05, was used to identify the different biomarkers between Cr0Se0 and Cr0Se5, Cr(III)200Se0 and Cr(III)200Se5, Cr(VI)120Se0 and Cr(VI)120Se0. Totally, 2 upregulated metabolites in Cr0Se5 vs. Cr0Se0 group (Table S1), 1 downregulated and 5 upregulated metabolites in Cr(III)200Se5 vs. Cr(III)200Se0 group, and 2 downregulated and 1 upregulated metabolites in Cr(VI)120Se5 vs. Cr(VI)120Se0 group showed significant diference (Table 1).

Table 1. Differential metabolites in rhizosphere soil in Cr(III)200Se5 vs Cr(III)200Se0 treatments, Cr(VI)120Se5 vs Cr(VI)120Se0 treatments.

Systems	Ionization mode	RT(s)	m/z	Metabolites	VIP	Fold change	*p*-value
Cr(III)	ESI(+)	86.93	114.09	Epsilon-Caprolactam	1.79	**0.19**	0.007**
	ESI(+)	205.68	179.07	4-Hydroxy-3-methoxycinnamaldehyde	1.03	**2.05**	0.005**
	ESI(-)	111.20	297.24	Cis-9,10-Epoxystearic acid	1.29	**2.18**	0.016*
	ESI(-)	770.54	179.06	Myo-Inositol	1.50	**1.81**	0.044*
	ESI(-)	77.50	285.21	Hexadecanedioic acid	1.22	**3.83**	0.049*
	ESI(-)	304.13	339.07	Aesculin	1.15	**1.77**	0.025*
Cr(VI)	ESI(+)	113.52	135.12	Perillyl alcohol	1.03	**0.51**	0.007**
	ESI(+)	328.92	236.11	Caffeine	1.21	**0.30**	0.024*
	ESI(-)	101.49	137.02	Salicylic acid	1.32	**1.59**	0.010*

* and ** represent that $p < 0.05$ and $p < 0.01$.

To show the shifts of rhizosphere organic chemicals components induced by Cr contamination, the one-way ANOVA (p-value < 0.05) of Cr(III)0Se0, Cr(III)100Se0, Cr(III)200Se0 were conducted. The result showed that 14 and 28 metabolites with a significant difference were identified in negative and positive ion mode, respectively (Fig. S1 and Fig. S2). There were 8 carboxylic acids and 4 carbohydrates downregulated in Cr(III) contaminated soil. In the group of Cr(VI)0Se0, Cr(VI)60Se0, Cr(VI)120Se0, 21 and 37 significantly different metabolites were obtained with p-value < 0.05 (Fig. S3 and Fig. S4) in negative and positive ion mode, respectively. There were 13 carboxylic acids upregulated and 10 carbohydrates downregulated in Cr(VI) contaminated soil. In the group of Cr(III)0Se5, Cr(III)100Se5, Cr(III)200Se5, 25 and 17 metabolites were identified to be significant different metabolites in negative and positive ion mode, respectively (Fig. S5 and Fig. S6). There were 7 carboxylic acids and 6 carbohydrates downregulated in Cr(III) contaminated soil with Se application. In the group of Cr(VI)0Se5, Cr(VI)60Se5, Cr(VI)120Se5, 37 and 38 metabolites were identified as significantly different metabolites in negative and positive ion mode, respectively (Fig. 1 and Fig. 2). There were 15 carboxylic acids upregulated and 16 carbohydrates downregulated in Cr(VI) contaminated soil with Se application.

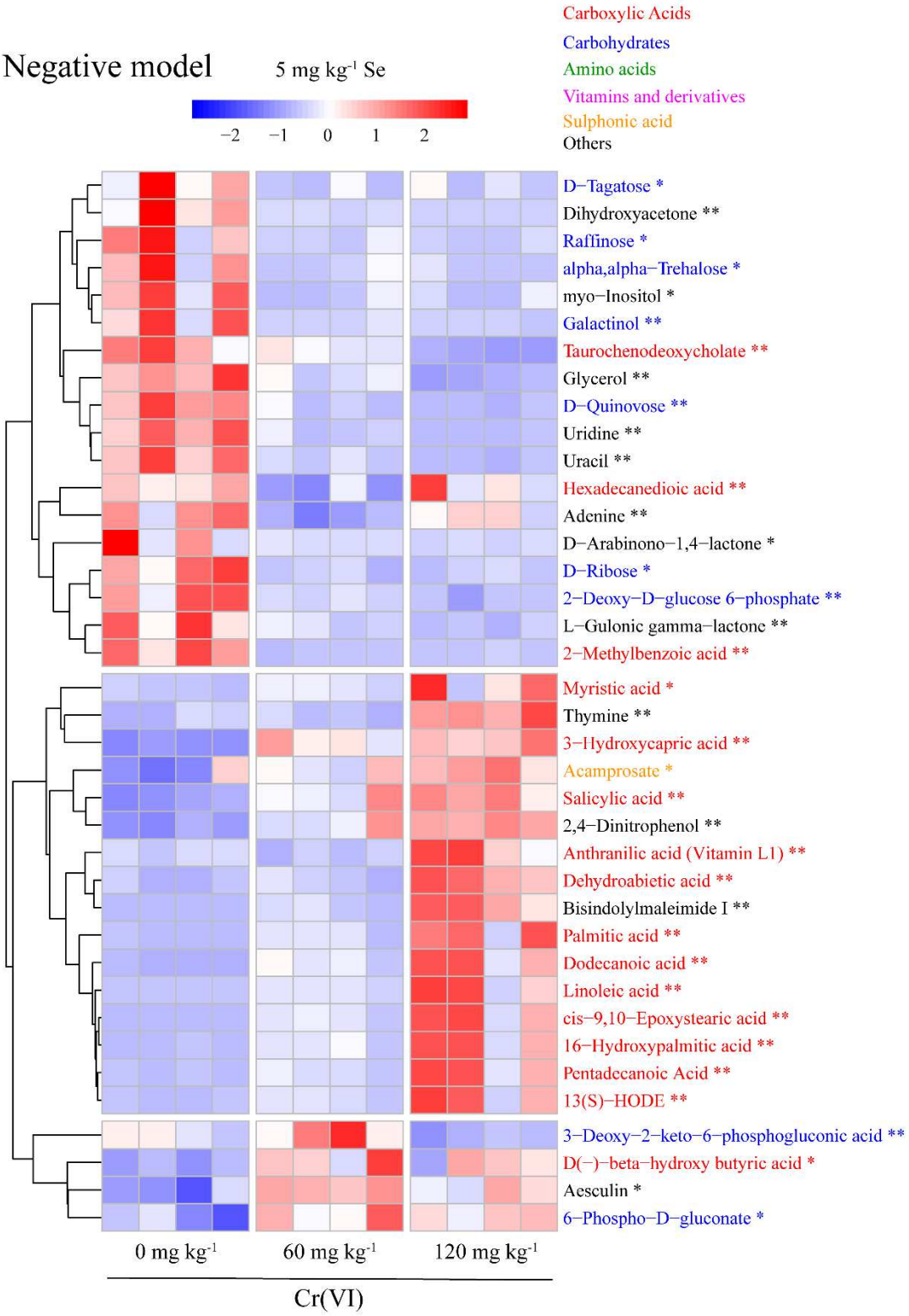

Fig. 1. Heatmap plot identifying significant difference ($p < 0.05$, negative model) between relative abundance of metabolites in Cr(VI) contaminated rhizosphere soils with Se application (5 mg kg^{-1}). Different color of metabolites means different categories. * and ** represent that $p < 0.05$ and $p < 0.01$.

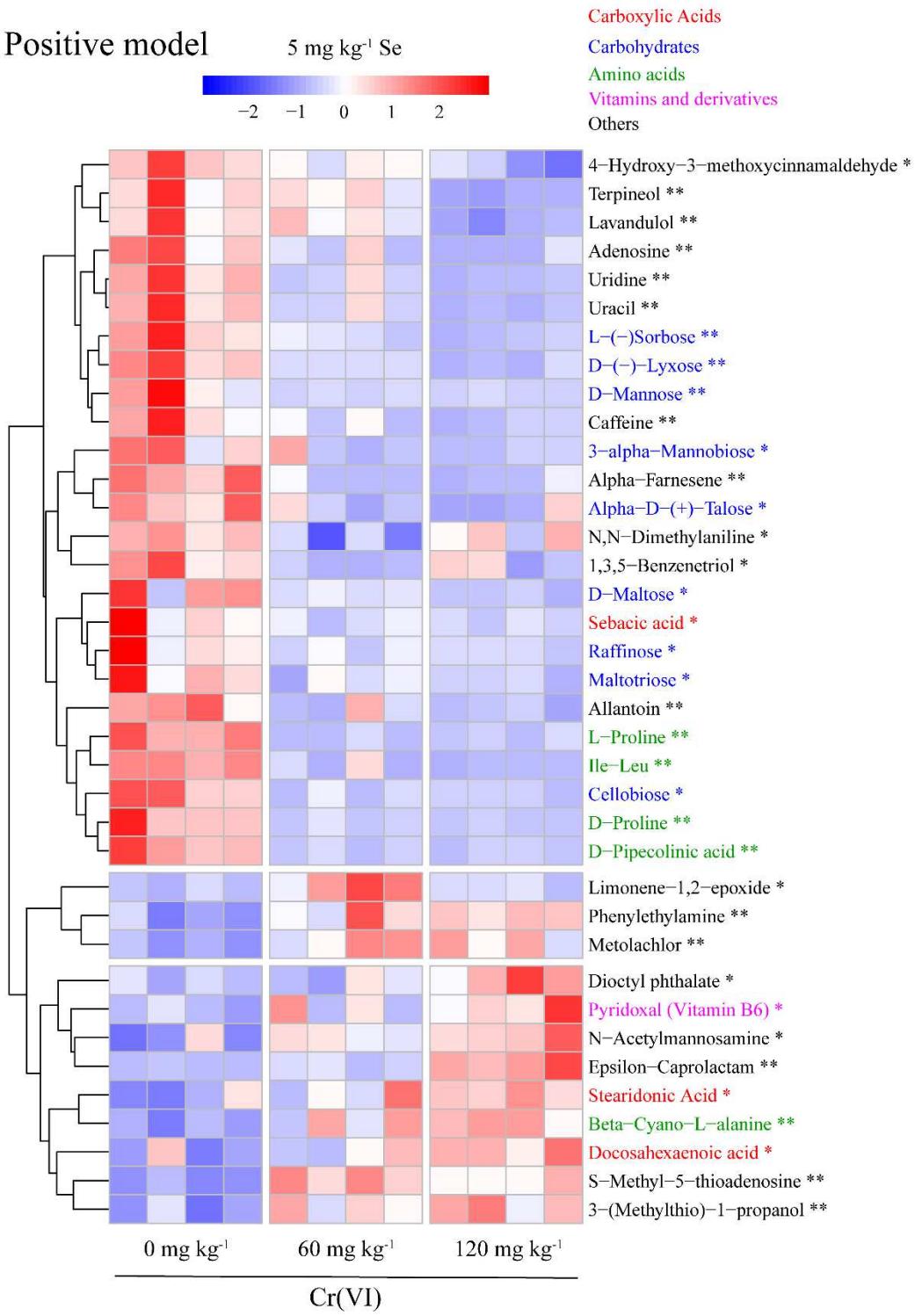

Fig. 2. Heatmap plot identifying significant difference ($p < 0.05$, positive model) between relative abundance of metabolites in Cr(VI) contaminated rhizosphere soils with Se application (5 mg kg^{-1}). Different color of metabolites means different categories. * and ** represent that $p < 0.05$ and $p < 0.01$.

3.2.Organic matter contents and its functional groups in Cr contaminated soil with Se application.

As shown in Fig. S7, the organic matter in RS and BS were significantly higher than that in CK without plant. But the quantities of organic matter showed no significant diference among diferent treatments.

Based on the FTIR spectra, the functional groups of the soil organic matter were presented. This supplement diferent insight into the composition of soil organic chemicals. Typical FTIR spectra of soils are presented in Fig. 3. According to literature, the absorption bands at 3433 cm^{-1} were assigned to -O-H and -N-H stretching vibration (Wen et al., 2018). A broad absorption mode in the 3000-2800 cm^{-1} region was the result of aliphatic C-H stretching vibration (Iqbal et al., 2009; Jia et al., 2018). The peaks at 1890 cm^{-1} and 1633 cm^{-1} attributed to N-O stretching vibration (Mihaylov et al., 2006) and C=O stretching vibration (Zhou et al., 2018; Liu et al. 2019b), respectively. The peak at 1385 cm^{-1} and 1033 cm^{-1} represented the result of COO- symmetric stretching of carboxylic acids (Amir et al., 2010) and C-O symmetric stretching of polysaccharose (Senesi et al., 2003; Yan et al., 2018) respectively. The absorption bands at 792 and 778 cm^{-1} were assigned to Si-O symmetric stretching in quartz (Chen et al., 2012). The peaks determined in the present study were similar. However, the peaks at 1385 cm^{-1} shifted to 1398-1400 cm^{-1} in Cr120Se0 and Cr120Se5 treatment soils (RS and BS). Similarly, the peaks at 1385 cm^{-1} shifted to 1387-1388 cm^{-1} in BS and shifted to 1398 cm^{-1} in RS with Cr200Se0 and Cr200Se5. The results indicated that COO-Cr complexes emerged in Cr contaminated soil. But the difference of the functional groups induced by Se application was not significant.

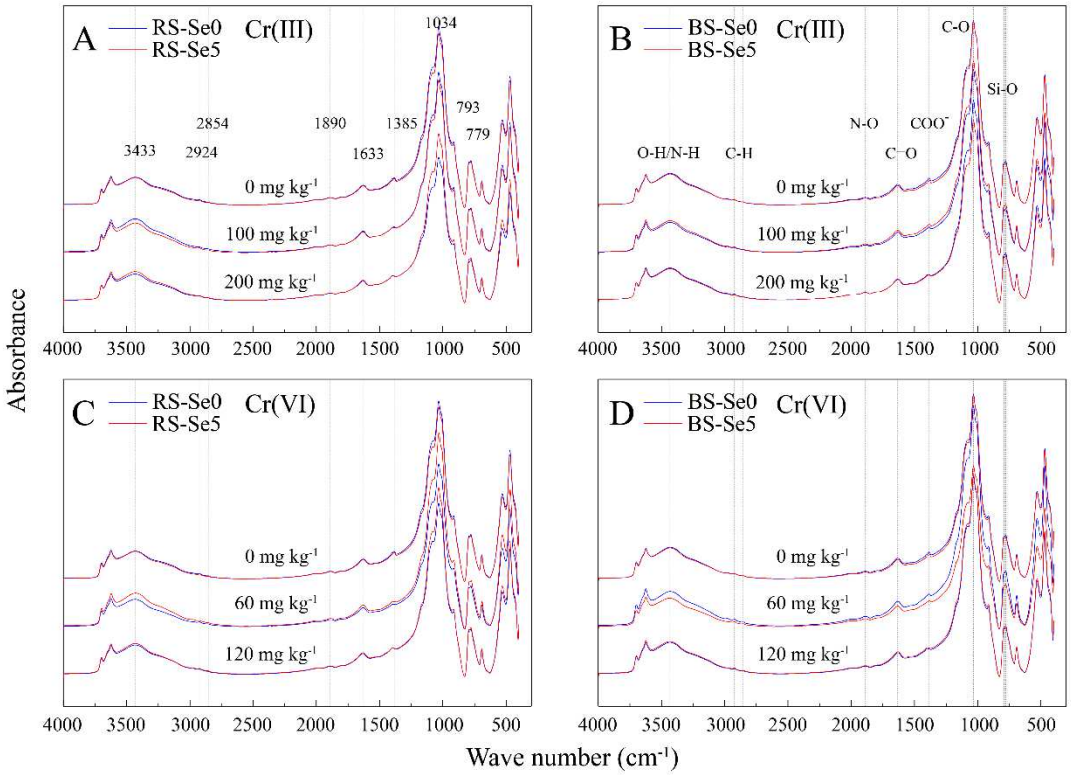

267

268

269 Fig. 3. FTIR spectra of Cr(III) contaminated soils (A: RS; B: BS) and Cr(VI) contaminated soils (C: RS;

270 D: BS) with and without Se application (5 mg kg^{-1}). RS: rhizosphere soils, BS: bulk soils.

3.3. Cr adsorption in soils with Se application and Se adsorption in Cr contaminated soil.

To evaluate the adsorption capacity of Cr/Se in soils, both Langmuir and Freundlich isotherm model (Dhillon and Dhillon, 1999; Fernández-Pazos et al., 2013; Choppala et al., 2018) were adopted in the present study.

To reveal the character of Cr absorption in soil with Se application, soil pretreated with Se (Cr0Se0, Cr0Se5) were used for Cr adsorption experiment. For Cr adsorption (Fig. 4), Freundlich isotherm model (R^2_{adj} > 0.982) was better fitted than Langmuir isotherm model (R^2_{adj} > 0.922). Moreover, the q_m of Langmuir isotherm model showed the elevated standard errors, indicating that the q_m was difficult to predict. Generally, according to the parameters in the Freundlich isotherm model, the higher k and n means the higher adsorption capacity. As a result, the adsorption capacity of RS was greater than the BS among all treatments. Furthermore, Se application (5 mg kg^{-1}) enhanced the adsorption capacity of Cr(III), however, it decreased that of Cr(VI) in RS.

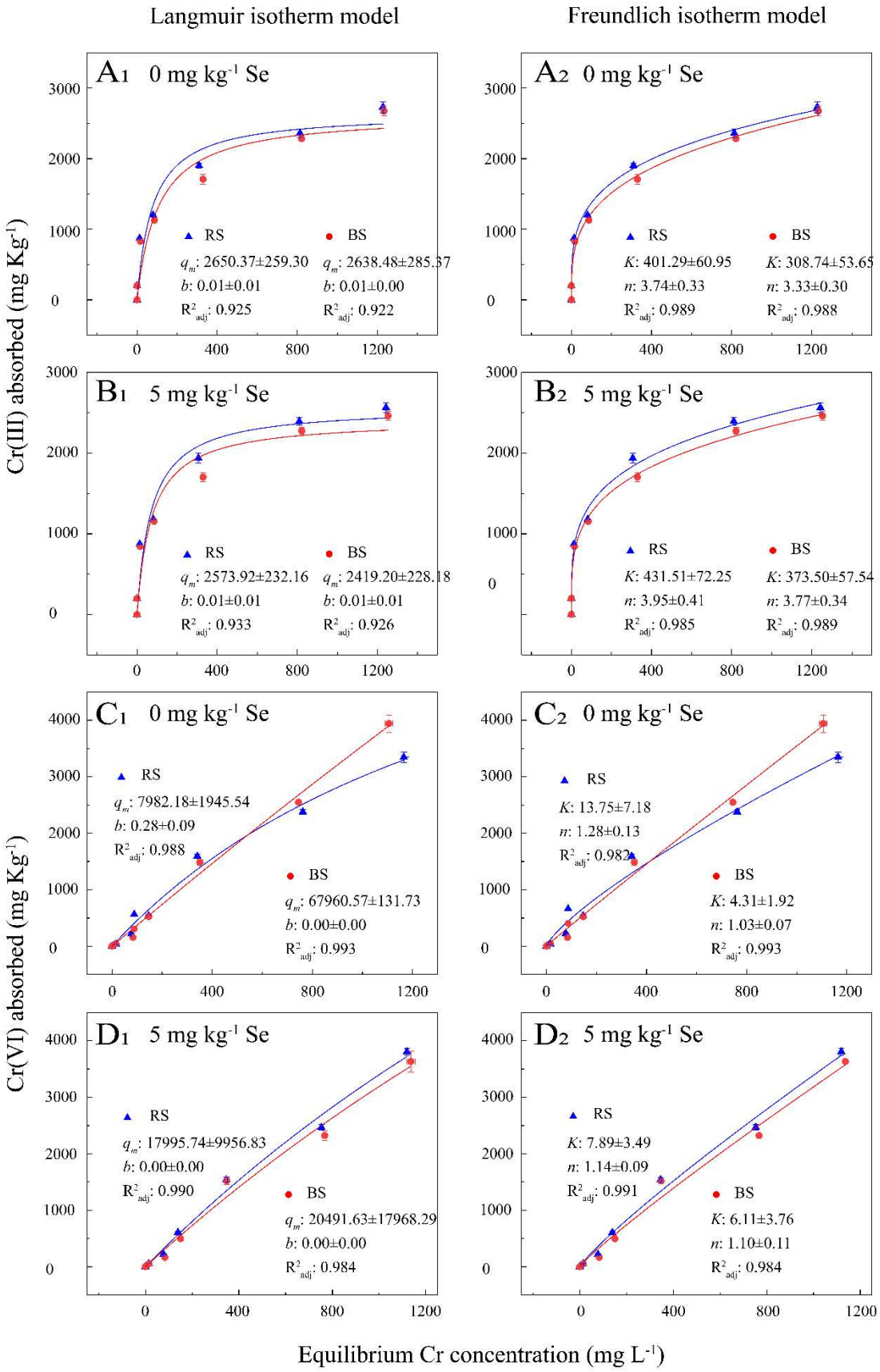

283

284 Fig. 4. Adsorption isotherm curves of Cr(III) and Cr(VI) in RS (rhizosphere soils, blue symbols and curves) and

BS (bulk soils, red symbols and curves), with or without Se application (5 mg kg^{-1}). Symbols represents experimental results, the error bars indicate the standard deviation; solid lines: fitting curves by Langmuir equation (A_1, B_1, C_1, D_1) and Freundlich equation (A_2, B_2, C_2, D_2).

To reveal the character of Se absorption in Cr contaminated soil, Cr contaminated soil (Cr0Se0, Cr(III)100Se0, Cr(VI)120Se0) were used for Se adsorption experiment. For Se adsorption (Fig. 5), both of Freundlich isotherm model ($R^2_{adj} > 0.992$) and Langmuir isotherm model ($R^2_{adj} > 0.984$) showed the good fitting. According to the Langmuir isotherm model, compared with no Cr contaminated soil, maximum sorption capacity of the soil (q_m) was lower and binding constant (b) was higher in Cr(III) contaminated soil (200 mg kg^{-1}), however, they were opposite in Cr(VI) contaminated soil (120 mg kg^{-1}). According to the Freundlich isotherm model, RS showed the higher k, indicating that the adsorption capacity of RS was greater than BS among all treatments. Furthermore, compared with no Cr contaminated soil, the parameter k, representing the adsorption capacity, in Cr(III) contaminated soil was greater, and it decreased in Cr(VI) contaminated soil.

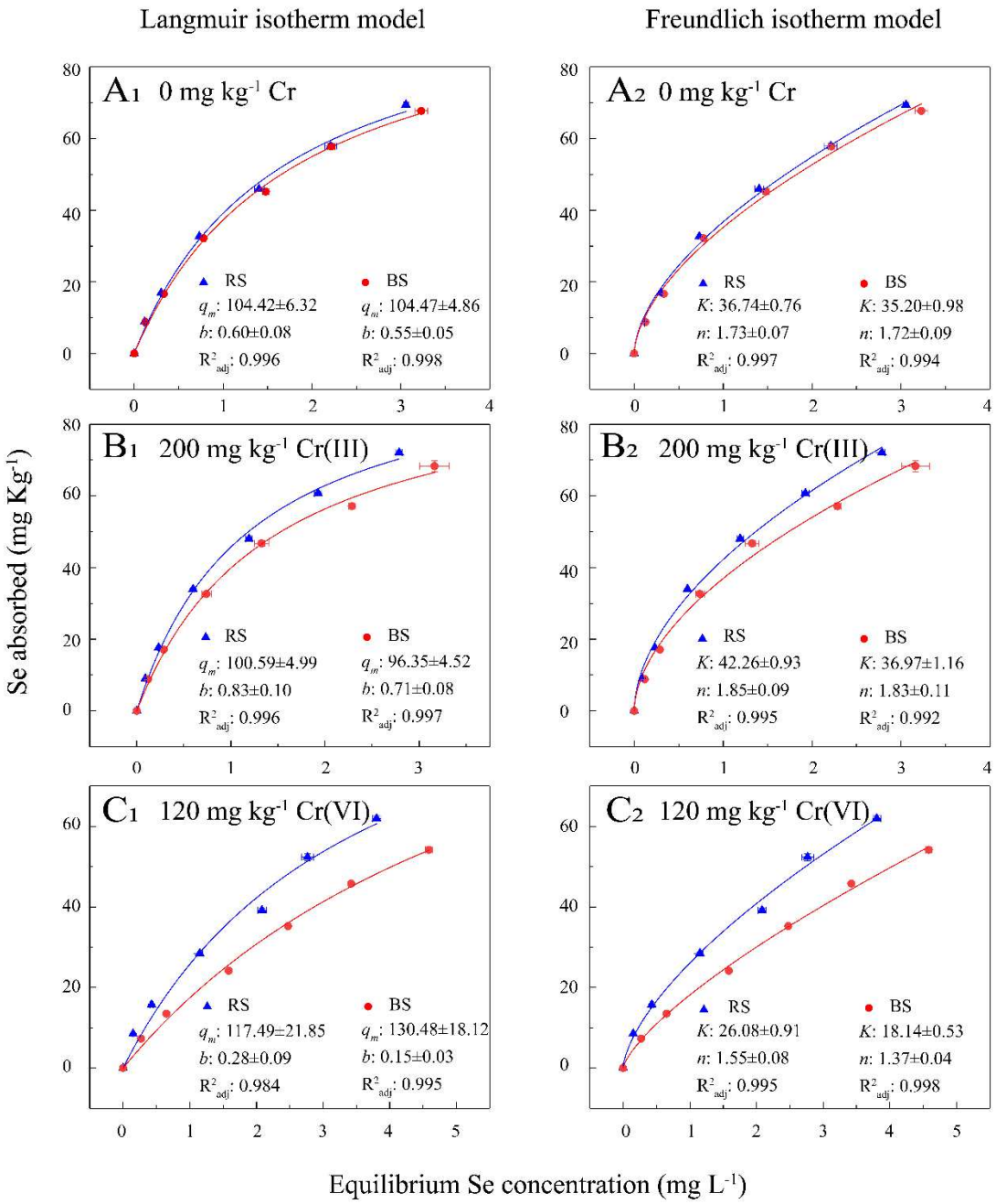

Fig. 5. Adsorption isotherm curves of Se in RS (rhizosphere soils, blue symbols and curves) and BS (bulk soils, red symbols and curves), without or with Cr contamination (Cr(III): 200 mg kg^{-1}; Cr(VI): 120 mg kg^{-1}). Symbols represents experimental results, the error bars indicate the standard deviation; solid lines: fitting curves by Langmuir equation (A1, B1, C1) and Freundlich equation (A2, B2, C2).

4. Discussion

In our previous study, it was found that Cr bioavailability decreased in Cr(III) contaminated soil and increased in Cr(VI) contaminated soil with Se application, and which were ascribed to the bacterial community

fluctuation (Cai et al., 2019). However, rhizosphere is a dynamic and highly complex ecosystem, including microbes, organic components and inorganic components. While, the rhizosphere organic chemicals mainly include root exudates, their breakdown products, and microbe products. In the present study, we focused on the rhizosphere organic components, its functional groups and the character of Cr adsorption. Totally, 79 metabolites in negative model and 85 metabolites in positive model were identified using UPLC-Q-TOF/MS analysis. In soils without Cr contamination, the increase of cellobiose release with Se application might be induced by carbohydrate metabolism in plant (Malik et al., 2011; Owusu-Sekyere et al., 2013). Moreover, based on the findings that polycarboxylates acted as electron transfer between Cr(VI) and weak electron donors to accelerate Cr(VI) reduction reported by Jiang et al. (2018), therefore, the enhance of cis-9,10-Epoxystearic acid and hexadecanedioic acid might act as electron transfer to reduce Cr(VI) to Cr(III), and then result in a decrease of Cr bioavailability with Se application in soil contaminated with 200 mg kg^{-1} Cr(III). When soil contaminated with 120 mg kg^{-1} Cr(VI), the increase of salicylic acid was observed with Se application. Salicylic acid was regarded as the antidote for plants under Cr stress (Huda, et al., 2016; Sihag et al., 2019), and it could complex with Cr(III) to increase Cr(III) mobility, thus enhancing Cr bioavailability in soil (Sun et al., 2000; Feijóo et al., 2010). However, according to the FTIR spectra, with or without Se application, the peaks at 1385 cm^{-1} (COO- symmetric stretching of carboxylic acids) shifted to 1396-1400 cm^{-1} with Cr(III)/(VI) contamination, and the results might be ascribed to the formation of metal complexation (Wen et al., 2018).

To reveal the character of Cr adsorption in soil with Se application, soil pretreated with Se (Cr0Se0, Cr0Se5) were used for Cr adsorption experiment. Based on the results of Cr adsorption, the adsorption capacity of RS was greater than that of BS. These results might be ascribed to the enriched organic matter. Findings of the current study were in line with the results reported by Jardine et al. (2013) that the sorption of Cr(VI) increased with the increasing total organic carbon in soil. Basically, Cr(III) existed as $Cr(OH)_2^+$ and Cr^{3+}, Cr(VI) existed as $HCrO_4^-$, $Cr_2O_7^{2-}$ (Shahid et al., 2017), and Se existed as $HSeO_3^-$, SeO_4^{2-} (Dinh et al., 2017) in the current soil pH range (4-6). Because of the formation of Se(IV)-Cr(III)-humic acid ternary complexes (Martin et al., 2017) and $Cr(III)_2(SeO_3)_3$ complexes (Srivastava et al., 1998), we inferred that Se(IV) complexed with Cr(III), therefore, Se addition decreased Cr bioavailability in Cr(III) contaminated soil. Moreover, because phosphate was identified as a strong competitor for Cr(VI) adsorption (Gu et al., 2017) and Se(IV) adsorption (Nakamaru et al., 2006), it could be inferred that Cr(VI) and Se(IV) competed for adsorption sites with each other and thus increased the Cr bioavailability in Cr(VI) contaminated soil.

Moreover, when Se was supplied, both Se accumulation in plant tissues and Se bioavailability in soil increased in soil with Cr contamination (Cai et al., 2019). In the present study, to explore factors regulated Se bioavailability is one of the subjects. The results of metabolomics showed that the relative abundance of carbohydrate decreased significantly, this might be mainly ascribed to the adverse effects on plant photosynthesis induced by Cr stress (Ali et al., 2013; Ma et al., 2016). The decrease of carbohydrate, which is the main food for microbe in soil, might decreased the microbe activities. Moreover, the carboxylic acids decreased in Cr(III) contaminated soil and increased in Cr(VI) contaminated soil. Udin et al. (2015) reported that the secretion of citric acid, malic acid and glutamic acid by *Solanum nigrum* L. and *Parthenium hysterophorus* L. plants increased significantly under Cr(VI) stress (500-1000 μmol L^{-1}). Zeng et al. (2008) reported that oxalic and malic acid were secreted by rice increased significantly under Cr(VI) stress (10-100 μmol L^{-1}), furtherly, the rhizosphere pH increased in this study. Similarly, the metabolites of microbe, such as exopolysaccharide and galacturonic acid, alginic acid, were affected by the Cr stress (Kılıç and Dönmez, 2008). As a supplementary, except for the bacterial community and soil pH (Cai et al., 2019), Se bioavailability were enhanced by the secretion of carboxylic acid. That might be ascribed to the synthesis effects of carboxylic acid on Se, including (i) reducing Se(VI) and Se(IV) to lower valent state, (ii) competing for the adsorption sites, (iii) formation of carboxylic acid-Se complex (Dinh et al., 2017).

To reveal the character of Se adsorption in Cr contaminated soil, Cr contaminated soil (Cr0Se0, Cr(III)100Se0, Cr(VI)120Se0) were used for Se adsorption experiment. Based on the results of Se adsorption, the adsorption capacity of RS was greater than that of BS. These results might be ascribed to the enriched organic matter. Similarly, Se(IV) sorption in soil positively correlated with organic matter content (Dhillon and Dhillon, 1999). Basically, Cr(III) existed as $Cr(OH)_2^+$ and Cr^{3+}, Cr(VI) existed as $HCrO_4^-$, $Cr_2O_7^{2-}$ (Shahid et al., 2017), and Se existed as $HSeO_3^-$, SeO_4^{2-} (Dinh et al., 2017) in the current soil pH range (4-6). Moreover, because phosphate was identified as a strong competitor for Cr(VI) adsorption (Gu et al., 2017) and Se(IV) adsorption (Nakamaru et al., 2006), it could be inferred that Cr(VI) and Se(IV) competed for adsorption sites with each other, and thus increased the Se bioavailability in soil.

5. Conclusions

In the current study, the rhizosphere organic chemicals regulated by Se/Cr contributed to the Cr/Se absorption character and bioavailability in soil. Moreover, the Cr/Se bioavailability and the adsorption capacity of soil were not only regulated by the quantity of the organic matter, but also by the categories and

functional groups of the organic profiles. Because the organic profiles can act as electron carriers, activators for the insoluble element and competitor for the adsorption site to regulate Cr/Se adsorption and bioavailability in soil. These results bettered our understanding of the rhizosphere processes related to the regulation of Cr/Se bioavailability in Cr contaminated soil. In the future, studying the response of rhizosphere dynamics in different types of soil with various plant species, is of great importance for exploring the potential role of Se accelerate cleaner production in soil contaminated by heavy metal.

Acknowledgments: This work is funded by the National Natural Science Foundation of China (41571321, 41807142), the Opening Project of Key Laboratory of Testing and Evaluation for Agro-product Safety and Quality, Ministry of Agriculture and Rural Affairs (NK201702), the Fundamental Research Funds for the Central Universities (2662018JC057), Hubei Provincial students' innovation and entrepreneurship training program (S201910504016).

Contributions

All authors contributed to the study conception and design. Miaomiao Cai: Conceptualization, Methodology, Visualization, Writting – original draft; Xu Wang, Guangyu Shi: Methodology, Investigation; Xiaohu Zhao: Conceptualization, Writting – review & editing, Supervision, Funding acquisition; Chengxiao Hu: Conceptualization, Writing – review & editing, Supervision. All authors read and approved the final manuscript.

Ethics declarations

Competing interests

The authors declare that they have no known competing interests.

Ethical approval and consent to participate

This manuscript does not report on or involve the use of any animal or human data or tissue, so it is not applicable in this section.

Consent to publish

This manuscript does not contain data from any individual person, so it is not applicable in this section.

Availability of data and materials

All data generated or analyzed during this study are included in this published article and its supplementary information files.

References

Ali, S., Farooq, M.A., Yasmeen, T., Hussain, S., Arif, M.S., Abbas, F., Bharwana, S.A., Zhang, G.P., 2013. The influence of silicon on barley growth, photosynthesis and ultra-structure under chromium stress. Ecotox. Environ. Safe. 89, 66-72.

Amir, S., Jouraiphy, A., Meddich, A., Gharous, M.E., Winterton, P., Hafidi, M., 2010. Structural study of humic acid during composting of activated sludge-green waste: Elemental analysis, FTIR and ^{13}C NMR. J. Hazard. Mater. 177, 524-529.

Bais, H.P., Weir, T.L., Perry, L.G., Gilroy, S., Vivanco, J.M., 2006. The role of root exudates in rhizosphere interactions with plants and other organisms. Annu. Rev. Plant Biol. 57, 233–66.

Bao, S.D., 2000. Soil agrochemical analysis. China Agriculture Press, Beijing.

Cai., M.M., Hu, C.X., Wang, X., Zhao, Y.Y., Jia, W., Sun, X.C., Elyamine, A.M., Zhao, X.H., 2019. Selenium induces changes of rhizosphere bacterial characteristics and enzyme activities affecting chromium/selenium uptake by pak choi (*Brassica campestris* L. ssp. *Chinensis* Makno) in chromium contaminated soil. Environ. Pollut. 249, 716–727.

Chen, K.Y., Liu, J.C., Chiang, P.N., Wang, S.L., Kuan, W.H., Tzou, Y.M., Deng, Y., Tseng, K.J., Chen, C.C., Wang, M.K., 2012. Chromate removal as influenced by the structural changes of soil components upon carbonization at different temperatures. Environ. Pollut. 162, 151-158.

Chen, Y.T., Wang, Y., Yeh, K.C., 2017. Role of root exudates in metal acquisition and tolerance. Curr. Opin. Plant Biol. 39, 66–72.

Choppala, G., Kunhikrishnan, A., Seshadri, B., Park, J.H., Bush, R., Bolan, N., 2018. Comparative sorption of chromium species as influenced by pH, surface charge and organic matter content in contaminated soils. J. Geochem. Explor. 184, 255-260.

Del Real, A.E.P., Silvan, J.M., de Pascual-Teresa, S., García-Gonzalo, P., Lobo, M.C., Pérez-Sanz, A., 2017. Role of the polycarboxylic compounds in the response of *Silene vulgaris* to chromium. Environ. Sci. Pollut. Res. 24, 5746-5756.

Dhillon, K.S., Dhillon, S.K., 1999. Adsorption–desorption reactions of selenium in some soils of India. Geoderma 93, 19–31.

Dinh, Q.T., Li, Z., Tran, T.A.T., Wang, D., Liang, D.L., 2017. Role of organic acids on the bioavailability of selenium in soil: A review. Chemosphere 184, 618-635.

Feijóo, A., Araujo, M.L., Brito, F., Lubes, G., Rodriguez, M., Lubes, V., 2010. Speciation of chromium(III)-salicylic acid system studied in 1.5 mol • dm^{-3} KCl at 25 ° C. J. Chem. Eng. Data 55, 4062-4065.

Fernández-Pazos, M.T., Garrido-Rodriguez, B., Nóvoa-Muñoz, J.C., Arias-Estévez, M., Fernández-Sanjurjo, M.J., Núñez-Delgado, A., Álvarez, E., 2013. Cr(VI) adsorption and desorption on soils and biosorbents. Water Air Soil Poll. 224, 1366.

Gu, X.Y., Xie, J.Y., Wang, X.R., Evans, L.J., 2017. A simple model to predict chromate partitioning in selected soils from China. J. Hazard. Mater. 322, 421-429.

Handa, N. Kohli, S.K., Sharma, A., Thukral, A.K., Bhardwaj, R., Alyemeni, M.N., Wijava, L., Ahmad, P., 2018a. Selenium ameliorates chromium toxicity through modifications in pigment system, antioxidative capacity, osmotic system, and metal chelators in *Brassica juncea* seedlings. S. Afr. J. Bot. 119, 1-10

Handa, N., Kohli, S.K., Thukral, A.K., Bhardwaj, R., Alyemeni, M.N., Wijaya, L., Ahmad, P., 2018b. Protective role of selenium against chromium stress involving metabolites and essential elements in *Brassica juncea* L. seedlings. 3 Biotech. 8, 66.

Huang, Q.Q., Xu, Y.M., Liu, Y.Y., Qin, X., Huang, R., Liang, X.F., 2018. Selenium application alters soil cadmium bioavailability and reduces its accumulation in rice grown in Cd-contaminated soil. Environ. Sci. Pollut. Res. 25, 31175-31182.

Huang, S.H., Peng, B., Yang, Z.H., Chai, L.Y., Zhou, L.C., 2009. Chromium accumulation, microorganism population and enzyme activities in soils around chromium-containing slag heap of steel alloy factory. Trans. Nonferrous Met. Soc. China 19, 241–248.

Huda, A.K.M.N., Swaraz, A.M., Reza, M.A., Haque, M.A., Kabir, A.H., 2016. Remediation of chromium toxicity through exogenous salicylic acid in rice (*Oryza sativa* L.). Water Air Soil Pollut. 227, 278.

Iqbal, M., Saeed, A., Zafar, S.I., 2009. FTIR spectrophotometry, kinetics and adsorption isotherms modeling, ion exchange, and EDX analysis for understanding the mechanism of Cd^{2+} and Pb^{2+} removal by mango peel waste. J. Hazard. Mater. 164, 161-171.

Ismael, M.A., Elyamine, A.M., Moussa, M.G., Cai, M.M., Zhao, X.H., Hu, C.X., 2019. Cadmium in plants: uptake, toxicity, and its interactions with selenium fertilizers. Metallomics 11, 255–277.

Jardine, P.M., Stewart, M.A., Barnett, M.O., Basta, N.T., Brooks, S.C., Fendorf, S., Mehlhorn, T.L., 2013. Influence of soil geochemical and physical properties on chromium(VI) sorption and bioaccessibility. Environ. Sci. Technol. 47, 11241-11248.

Jia, W., Hu, C.X., Ming, J.J., Zhao, Y.Y., Xin, J., Sun, X.C., Zhao, X.H., 2018. Action of selenium against *Sclerotinia sclerotiorum*: Damaging membrane system and interfering with metabolism. Pestic. Biochem. Phys. 150, 10-16.

Jiang, B., He, H.H., Liu, Y.J., Tang, Y.Z., Luo, S.Y., Wang, Z.H., 2018. pH-dependent roles of polycarboxylates in electron transfer between Cr(VI) and weak electron donors. Chemosphere 197, 367-374.

Kılıç, N.K., Dönmez, G., 2008. Environmental conditions affecting exopolysaccharide production by *Pseudomonas aeruginosa*, *Micrococcus* sp., and *Ochrobactrum* sp. J. Hazard. Mater. 154, 1019-1024.

Lei, L., Zhu, J.M., Wang, F.P., Xiao, X., Qin, H.B., Feng, X.B., 2011. Primarily investigating the diversity of microorganisms in selenium-rich carbonaceous mudstone of Yutangba, Enshi, Hubei. Earth Environ. (Chinese) 39 (4), 517-522.

Liu, K., Cai, M.M., Hu, C.X., Sun, X.C., Cheng, Q., Jia, W., Yang, T., Nie, M., Zhao, X.H., 2019a. Selenium (Se) reduces Sclerotinia stem rot disease incidence of oilseed rape by increasing plant Se concentration and shifting soil microbial community and functional profiles. Environ. Pollut. 254, 113051.

Liu, Q.J., Li, X., Tang, J.P., Zhou, Y.M., Lin, Q.T., Xiao, R.B., Zhang, M., 2019b. Characterization of goethite-fulvic acid composites and their impact on the immobility of Pb/Cd in soil. Chemosphere 222, 556-563.

Ma, J., Lv, C.F., Xu, M.L., Chen, G.X., Lv, C.G., Gao, Z.P., 2016. Photosynthesis performance, antioxidant enzymes, and ultrastructural analyses of rice seedlings under chromium stress. Environ. Sci. Pollut. Res. 23 (2): 1768-1778.

Malik, J.A., Kumar, S., Thakur, P., Sharma, S., Kaur, N., Kaur, R., Pathania, D., Bhandhari, K., Kaushal, N., Singh, K., Srivastava, A., Nayyar, H., 2011. Promotion of growth in mungbean (*Phaseolus aureus* Roxb.) by selenium is associated with stimulation of carbohydrate metabolism. Biol. Trace Elem. Res. 143, 530-539.

Martin, D.P., Seiter, J.M., Lafferty, B.J., Bednar, A.J., 2017. Exploring the ability of cations to facilitate binding between inorganic oxyanions and humic acid. Chemosphere 166, 192-196.

Mihaylov, M., Penkova, A., Hadjiivanov, K., Daturi, M., 2006. Chromium nitrosyl complexes in Cr-ZSM-5: An FTIR spectroscopic study. J. Mol. Catal. A-Chem. 249, 40-46.

Nakamaru, Y., Tagami, K., Uchida, S., 2006. Effect of phosphate addition on the sorption-desorption reaction of selenium in Japanese agricultural soils. Chemosphere 63, 109-115.

Owusu-Sekyere, A., Kontturi, J., Hajiboland, R., Ranmat, S., Aliasgharzad, N., Hartikainen, H., Seppanen, M.M., 2013. Influence of selenium (Se) on carbohydrate metabolism, nodulation and growth in alfalfa (*Medicago sativa* L.). Plant Soil 373, 541-552.

Pétriacq, P., Williams, A., Cotton, A., McFarlane, A.E., Rolfe, S.A., Ton, J., 2017. Metabolite profiling of non−sterile rhizosphere soil. Plant J. 92, 147–162.

Qing, X.J., Zhao, X.H., Hu, C.X., Wang, P., Zhang, Y., Zhang, X., Wang, P.C., Shi, H.Z., Jia, F., Qu, C.J., 2015. Selenium alleviates chromium toxicity by preventing oxidative stress in cabbage (*Brassica campestris* L. ssp. *Pekinensis*) leaves. Ecotox. Environ. Safe. 114, 179–189.

Rosenfeld, C.E., James, B.R., Santellia, C.M., 2018. Persistent bacterial and fungal community shifts exhibited in selenium-contaminated reclaimed mine soils. Appl. Environ. Micro. 84 (6), e01394–18.

Senesi, N., D'Orazio, V., Ricca, G., 2003. Humic acids in the first generation of EUROSOILS, 2003. Geoderma 116, 325-344.

Shahid, M., Shamshad, S., Rafiq, M., Khalid, S., Bibi, I., Niazi, N.K., Dumat, C., Rashid, M.I., 2017. Chromium speciation, bioavailability, uptake, toxicity and detoxification in soil-plant system: A review. Chemosphere 178, 513–533.

Sihag, S., Brar, B., Joshi, U.N., 2019. Salicylic acid induces amelioration of chromium toxicity and affects antioxidant enzyme activity in *Sorghum bicolor* L. Int. J. Phytoremediat. 21 (4): 293-304.

Srivastava, S., Shanker, K., Srivastava, Sh., Shrivastav, R., Das, S., Prakash, S., Srivastava, M.M., 1998. Effect of selenium supplementation on the uptake and translocation of chromium by Spinach (*Spinacea oleracea*). Bull. Environ. Contam. 60, 750–758.

Sun, Y.J., Ramirez, J., Woski, S.A., Vincent, J.B., 2000. The binding of trivalent chromium to low-molecular-weight chromium-binding substance (LMWCr) and the transfer of chromium from transferrin and chromium picolinate to LMWCr. JBIC 5, 129-136.

Udin, I., Bano, A., Masood, S., 2015. Chromium toxicity tolerance of *Solanum nigrum* L. and *Parthenium hysterophorus* L. plants with reference to ion pattern, antioxidation activity and root exudation. Ecotox. Environ. Safe. 113, 271-278.

Van Dam, N.M., Bouwmeester, H.J., 2016. Metabolomics in the rhizosphere: tapping into belowground chemical communication. Trends Plant Sci. 21 (3), 256-265.

Wang, Y.J., Dang, F., Evans, R.D., Zhong, H., Zhao, J., Zhou, D.M., 2016. Mechanistic understanding of MeHg-Se antagonism in soil rice systems: the key role of antagonism in soil. Sci. Reo. 6: 19477.

Wen, J.J., Li, Z.W., Huang, B., Luo, N.L., Huang, M., Yang, R., Zhang, Q., Zhai, X.Q., Zeng, G.M., 2018. The complexation of rhizosphere and nonrhizosphere soil organic matter with chromium: Using elemental analysis combined with FTIR spectroscopy. Ecotox. Environ. Safe. 154, 52-58.

Wen, X., Hu, Y.D., Zhang, X.Y., Wei, X.Z., Wang, T., Yin, S.W., 2019. Integrated application of multi-omics provides insights into cold stress responses in pufferfish *Takifugu fasciatus*. BMC Genomics 20, 563.

Yan, L., Riaz, M., Wu, X.W., Du, C.Q., Liu, Y.L., Jiang, C.C., 2018. Ameliorative effects of boron on aluminum induced variations of cell wall cellulose and pectin components in trifoliate orange (*Poncirus trifoliate* (L.) Raf.) rootstock. Environ. Pollut. 240, 764-774.

Yang, S.Y., Zhao, J., Chang, S.X., Collins, C., Xu, J.M., Liu, X.M., 2019. Status assessment and probabilistic health risk modeling of metals accumulation in agriculture soils across China: A synthesis. Environ. Int. 128, 165–174.

Zeng, F.R., Chen, S., Miao, Y., Wu, F.B., Zhang, G.P., 2008. Changes of organic acid exudation and rhizosphere pH in rice plants under chromium stress. Environ. Pollut. 155, 284–289.

Zhalnina, K., Louie, K.B., Hao, Z., Mansoori, N., da Rocha, U.N., Shi, S.J., Cho, H., Karaoz, U., Loqué, D., Bowen, B.P., Firestone, M.K., Northen, T.R., Brodie, E.L., 2018. Dynamic root exudate chemistry and microbial substrate preferences drive patterns in rhizosphere microbial community assembly. Nat. Microbiol. 3, 470–480.

Zhao, Y.Y., Hu, C.X., Wang, X., Qing, X.J., Wang, P., Zhang, Y., Zhang, X., Zhao, X.H., 2019a. Selenium alleviated chromium stress in Chinese cabbage (*Brassica campestris* L. ssp. *Pekinensis*) by regulating root morphology and metal element uptake. Ecotox. Environ. Safe. 173, 314–321.

Zhao, Y.Y., Hu, C.X., Wu, Z.C., Liu, X.W., Cai, M.M., Jia, W., Zhao, X.H., 2019b. Selenium reduces cadmium accumulation in seed by increasing cadmium retention in root of oilseed rape (Brassica napus L.). Environ. Exp. Bot. 158, 161–170.

Zhou, T., Wu, L.H., Luo, Y.M., Christie, P., 2018. Effects of organic matter fraction and compositional changes on distribution of cadmium and zinc in long-term polluted paddy soils. Environ. Pollut. 232, 514-522.

Zwetsloot, N.J., Kessler, A., Bauerle, T.L., 2018. Phenolic root exudate and tissue compounds vary widely among temperate forest tree species and have contrasting effects on soil microbial respiration. New Phytol. 218 (2), 530–541.

Figures

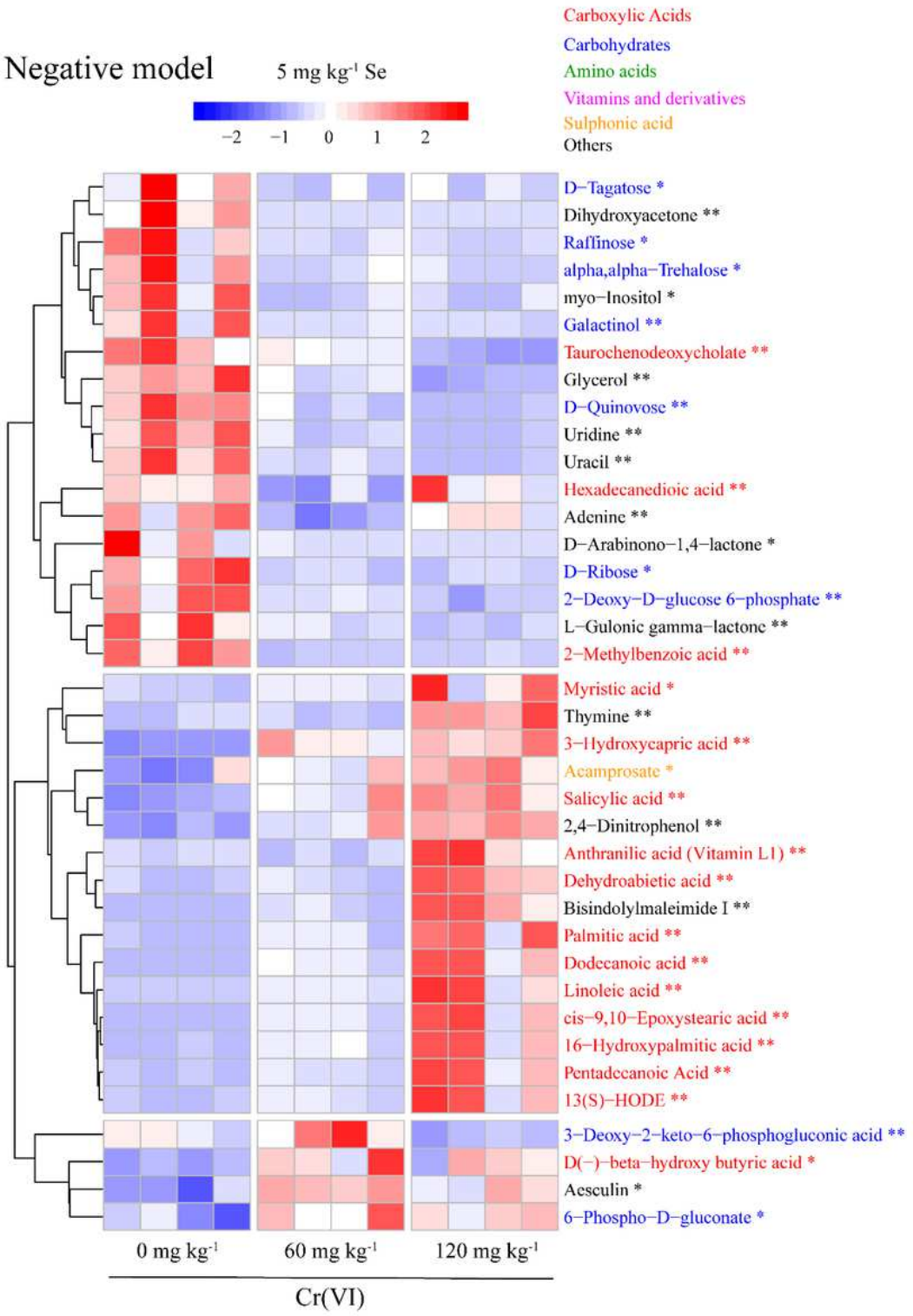

Figure 1

Heatmap plot identifying significant difference ($p < 0.05$, negative model) between relative abundance of metabolites in Cr(Ⅵ) contaminated rhizosphere soils with Se application (5 mg kg-1). Different color of metabolites means different categories. * and ** represent that $p < 0.05$ and $p < 0.01$.

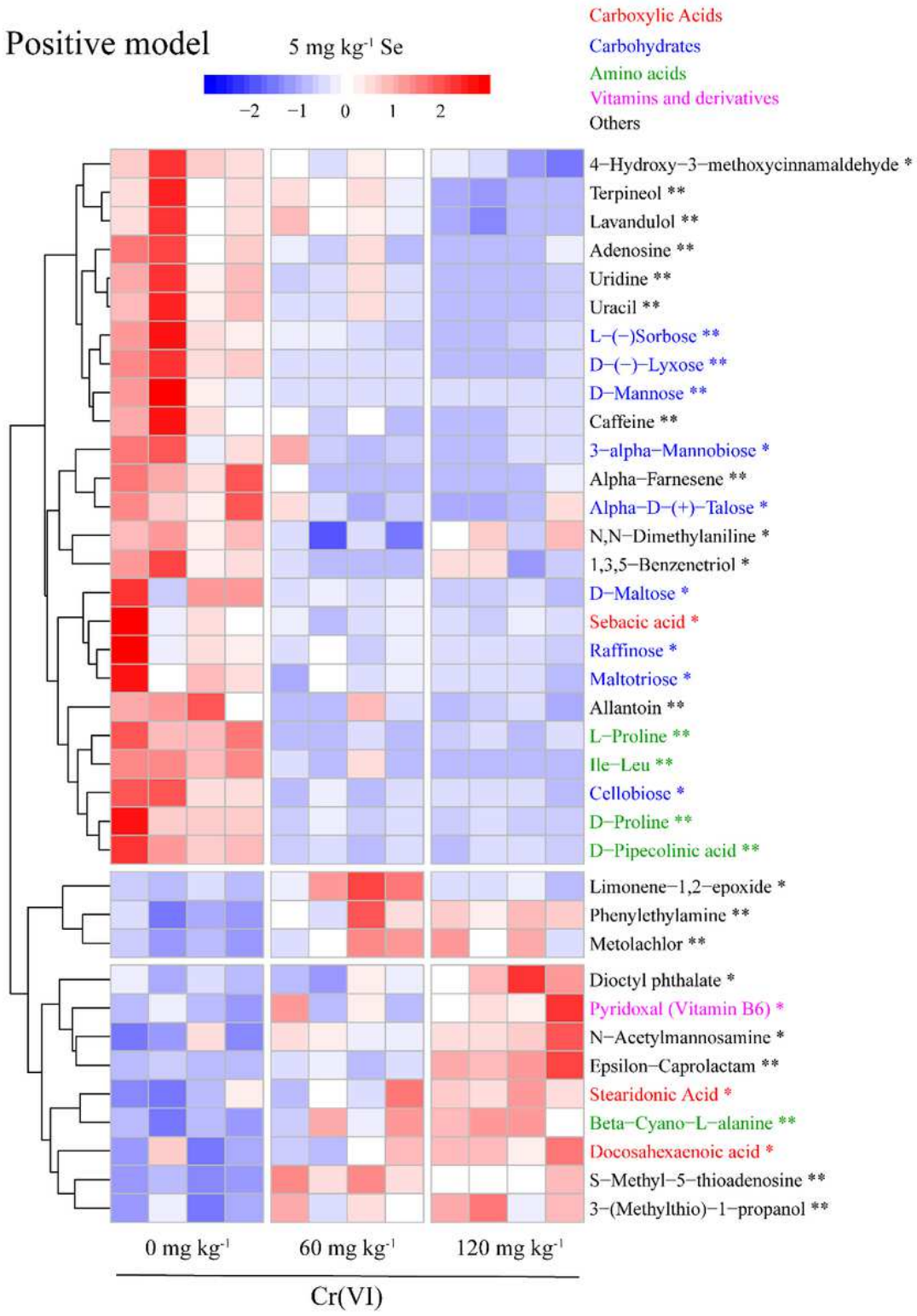

Figure 2

Heatmap plot identifying significant difference ($p < 0.05$, positive model) between relative abundance of metabolites in Cr(□) contaminated rhizosphere soils with Se application (5 mg kg-1). Different color of metabolites means different categories. * and ** represent that $p < 0.05$ and $p < 0.01$.

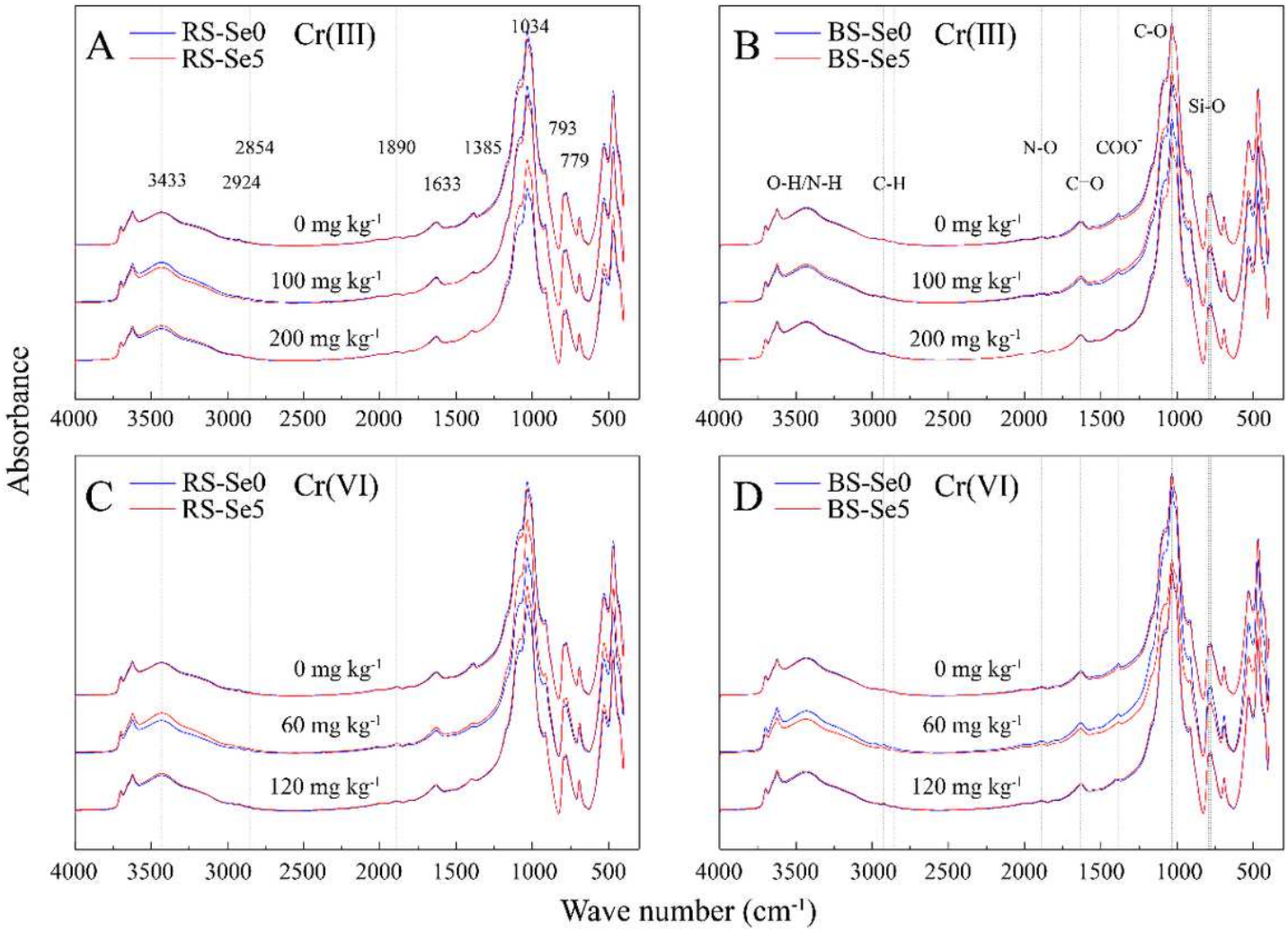

Figure 3

FTIR spectra of Cr(□) contaminated soils (A: RS; B: BS) and Cr(□) contaminated soils (C: RS; D: BS) with and without Se application (5 mg kg-1). RS: rhizosphere soils, BS: bulk soils.

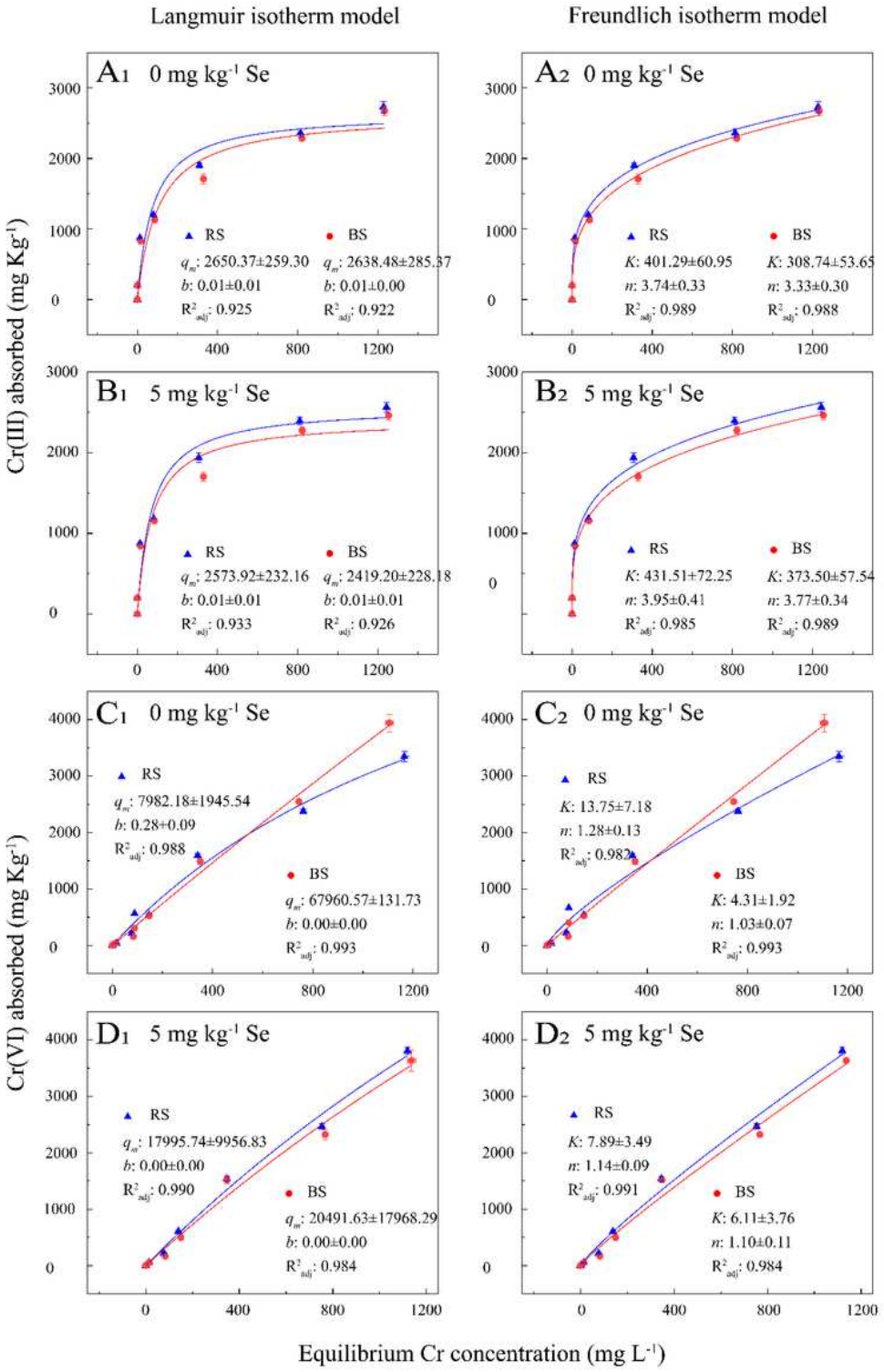

Figure 4

Adsorption isotherm curves of Cr(Ⅲ) and Cr(Ⅵ) in RS (rhizosphere soils, blue symbols and curves) and BS (bulk soils, red symbols and curves), with or without Se application (5 mg kg-1). Symbols represents experimental results, the error bars indicate the standard deviation; solid lines: fitting curves by Langmuir equation (A1, B1, C1, D1) and Freundlich equation (A2, B2, C2, D2).

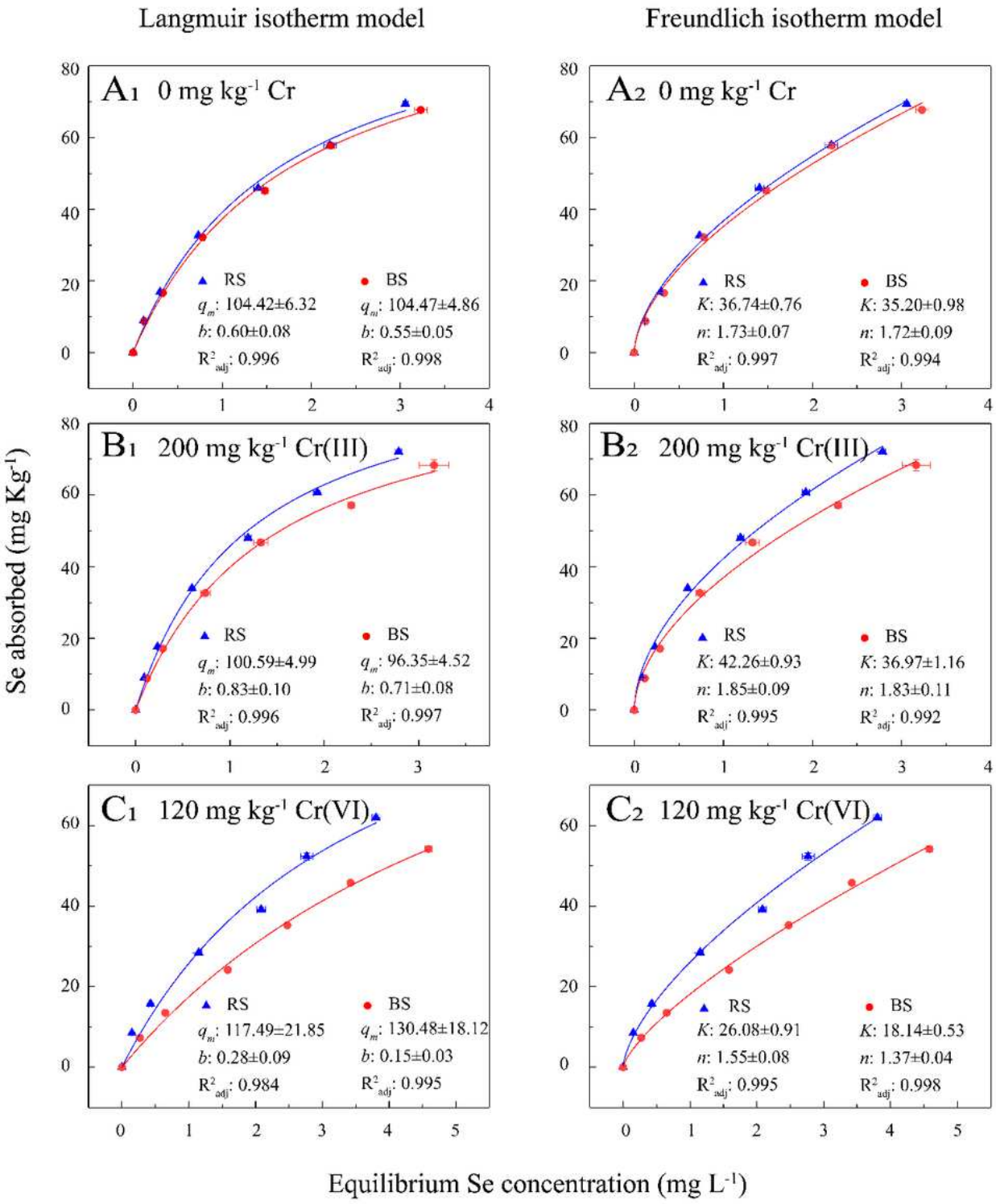

Figure 5

Adsorption isotherm curves of Se in RS (rhizosphere soils, blue symbols and curves) and BS (bulk soils, red symbols and curves), without or with Cr contamination (Cr(□): 200 mg kg-1; Cr(□): 120 mg kg-1). Symbols represents experimental results, the error bars indicate the standard deviation; solid lines: fitting curves by Langmuir equation (A1, B1, C1) and Freundlich equation (A2, B2, C2).

Supplementary Files

This is a list of supplementary files associated with this preprint. Click to download.

- SupplementaryInformation.docx